Hindawi
Mathematical Problems in Engineering
Volume 2020, Article ID 9406479, 10 pages
https://doi.org/10.1155/2020/9406479

Research Article

A Novel Median-Point Mode Decomposition Algorithm for Motor Rolling Bearing Fault Recognition

Ganzhou Yao, Bishuang Fan, Wen Wang, and Haihang Ma

School of Electrical and Information Engineering, Changsha University of Science & Technology, Changsha, China

Correspondence should be addressed to Bishuang Fan; fbs@csust.edu.cn

Received 31 July 2020; Accepted 13 September 2020; Published 16 November 2020

Academic Editor: Yong Chen

Precise fault recognition of motor rolling bearing fault is playing a significant role in any machinery and equipment. However, conventional decomposition methods fail to completely reveal the fault signal information of motor rolling bearing due to mixed modes problem. To solve the problem, the median-point mode decomposition (MMD) method is presented. The MMD method uses sort-based inversion to sort out each variation of the same time interval for better and specific mode decomposition, with the assistance of the advanced envelope curve formed by the median points between adjacent extreme points. It certainly alleviates the mixed mode during the iteration of intrinsic mode functions (IMFs). Therefore, comparison results are simulated in the proposed MMD method with conventional methods. Experiment of motor rolling bearing fault is operated for fault recognition in order to demonstrate the MMD algorithm.

1. Introduction

Rolling bearings are common components in rotating machines, which have been significant in the industry. The motor signal is a nonlinear, nonstationary weak signal with strong randomness. In the acquisition process, it will be affected by external environmental actions or noise interference such as power frequency, leading to mixed modes in the IMF components. Therefore, the preprocessing of this type of signal is an important research problem. Meanwhile, fault signal of the motor cannot be intuitively observed due to its characteristic complexity, so it needs to be decomposed or extracted in time domain and frequency domain and fault characteristic values from multiple angles should be obtained. Feature extraction is the core content of fault recognition. The accuracy of the signal process and that of feature extraction will directly affect the reliability of fault recognition. Thus, HHT is an adaptive time-frequency analysis method to be used in the feature extraction of fault recognition.

Conventional signal processing techniques can only detect stationary and linear signals [1]. Wavelet transform was studied for nonstationary signals and time-sfrequency analysis [2], but the wavelet base function limits the result of it, which may lead to a priori assumption on the characteristics of the investigated vibration signal [3]. As a self-adaptive signal processing method, empirical mode decomposition (EMD) is analyzed to decompose the complicated signal into a set of complete and intrinsic mode functions (IMFs) [4, 5].

However, mixed mode problem is one of the major drawbacks of EMD, caused by the screening process in the EMD algorithm and the discontinuity of the eigenmode function of a certain time scale and several time scales [6]. Mixed mode problem leads to the decomposed IMFs becoming distorted because the signals are mixed with discontinuous high-frequency weak noise interference and it confuses the time-frequency distribution, making each IMF lack physical meaning.

A simple mixed mode example would be like two identical signals, one having low-order random noise and the other not; the results of EMD decomposition can be quite different [7–10]. Mixed modes in bearing faults cause the fatal breakdown of machines and inestimable economic losses [11–14]. In order to overcome the above problems, ensemble empirical mode decomposition (EEMD) is studied

as a new solution for mixed mode problem, which is through adding finite white noise to the investigated signal. However, the Gaussian white noise may make it difficult to determine an ensemble mean as the different iterations can generate different number of IMFs [15–18]. Furthermore, the EEMD method is hard to be self-adaptive as it requires an amplitude of noise and ensemble number as parameters. Therefore, it is significant to detect the existence and severity of a bearing fault with an efficiently fast, accurate method.

In this paper, a novel median-point algorithm with time interval sort-based inversion is developed. EMD and EEMD algorithms with some of their drawbacks are reviewed. The rest of the paper is organized as follows: In Section 2, the principle of the proposed median-point mode decomposition is presented. Then, detail process simulations of MMD are shown in Section 3, followed by the flowchart of the MMD method. Finally, simulations of EMD and EEMD based on the same original mode as MMD and simulated fault recognition are all given to demonstrate that the proposed method based on MMD obtains a more precise mode decomposition result. The proposed MMD method can be applied in practice, particularly in fault recognition of rolling element bearings since its occurrence.

2. Principle of the Proposed Median-Point Mode Decomposition (MMD)

Median-point mode decomposition (MMD) can be treated as a screening process, which is a self-adaptive method and can decompose any complex signal into a list of intrinsic mode functions (IMFs), which must meet two conditions as follows in Table 1.

All the local extrema are identified as $x(t)$. In EMD, the first step is to construct the upper envelope and lower envelope in the signal by interpolating the local maxima and minima, respectively, using cubic spline [11]. However, in MMD, we apply sort-based inversion to detect out all periods in the same frequency and then, respectively, employ only the median point between adjacent extreme points of one specific part, to gain the median-point-fit-curve $m(t)$ for further managements.

Huge difference among EMD, EEMD, and MMD is that the sort-based inversion algorithm is adopted in MMD to sort the obtained time intervals from small to large. Set a default maximum value rate of time intervals earlier. Then, when the rate of change exceeds the set value, the system defaults to take the time interval value before the change as the maximum time interval value $T_{\max}$ of this required mode.

The median-point-fit-curve is formed by cubic spline function, under two different conditions, listed in Table 2.

Thus, the difference between the local extrema of $x(t)$ and median-point-fit-curve m(t) is marked as equation (1), which should meet the condition in Table 1:

$$h(t) = x(t) - m(t). \tag{1}$$

Repeat the above steps until $h(t)$ is an IMF, and then, set $c_i(t) = h(t)$. Then, compute the residue $r_i(t) = x(t) - c_i(t)$ and set $x(t) = r_i(t)$ and repeat the above steps to extract the next IMF until $r_i(t)$ is monotonic or constant.

The result of MMD algorithm can be expressed as

$$x(t) = \sum_{j=1}^{n} c_j(t) + r_n(t), \tag{2}$$

where $x(t)$ is decomposed into a series of IMFs $c_j(t)$ and a residue $r(t)$. For better presentation of the principle of MMD, we have listed the steps of MMD, as shown in Table 3.

3. Detail Process of MMD

The original signal composed of signals with different amplitude and frequency ratios is crucial to the EMD\EEMD mode mixing problems. As the principle of MMD is presented completely in Section 2, an example is presented as follows, where $x(t)$ is composed of x_1, x_2, x_3, x_4, and x_5:

$$x_1(t) = 0.01t, \tag{3}$$

$$x_2(t) = 0.1\sin(2\pi t), \tag{4}$$

$$x_3(t) = 0.12\sin(6\pi t), \tag{5}$$

$$x_4(t) = 0.15\sin(16\pi t_2), \tag{6}$$

$$x_5(t) = 0.35\sin(76\pi t_1), \tag{7}$$

where $0 \le t \le 2$, $0.3 \le t_2 \le 0.6$, and $1.3 \le t_1 \le 1.6$, shown in Figure 1.

The original signal $x(t)$ consists of constituent signals with different degrees of frequency separation, which is shown in Figure 1. Mixed mode exists in nonlinear and nonstationary signals. In order to verify the sensitivity of MMD to signal changes, the proposed method adds new interference processing in the time $t_1 = 0.3$ s and $t_2 = 1.3$ s and ends at the time of 0.6 s and 1.6 s, respectively. Each component in $x(t)$ contains only a simple vibration mode (single instantaneous frequency), and the signals of these components can completely represent the real physical information in the original signal.

For comparison, the simulation signal $x(t)$ is analyzed using the EMD and EEMD method and the decomposition results are displayed in Figures 2 and 3.

Notice that when EMD is operated on the original signal $x(t)$, the result is as shown in Figure 2. Mixed mode problem makes the scale of the first-order IMF1 (c_1) different, and the scale of IMF2 (c_2) is also affected by c_2, while c_3 and c_4 contain the same scale signal. It can be judged that there are obvious mixed modes existing, leading to the mode component becoming seriously distorted, as compared with the original signal. It is indistinct that the problem of mixed modes appears at IMF1-4 below, showing that the EMD method fails to provide the reasonable decomposition.

The components y_1, y_2, y_3, y_4, and y_5 in original signal $x(t)$ are defined in (equations (3)–(7)). From top to the bottom of Figure 2, each subfigure represents IMFs with ascending order and is produced by the EMD method.

Table 1: Conditions of IMF.

Condition 1	The number of signal extreme points is equal to zero point or the difference in them is within 1.
Condition 2	At any point, the mean value of the envelope defined by the local maxima and the envelope defined by the local minima is zero.

Table 2: Conditions of the maximum time interval value T_{max}.

Condition 1	When the interval of adjacent extreme points is larger than T_{max}, the value of median point would be the magnitude and amount of time of $x(t)$ between the current extreme points.
Condition 2	When the interval is less than T_{max}, the MMD assigns the value of median point from the current adjacent extreme points and the value of median point corresponding to the original signal, together to the value of median point.

Table 3: The MMD algorithm.

Step 1	Identify all the local extrema of $x(t)$.
Step 2	Obtain the local maxima and minima of $x(t)$.
Step 3	Gain all the time intervals between adjacent extreme points.
Step 4	Apply sort-based inversion algorithm for time intervals from high frequency to low.
Step 5	Determine the rate of change of the time interval and set a maximum of time interval T_{max}.
Step 6	Gain different values of median point in different periods of time intervals based on two conditions of T_{max}.
Step 7	In each sorted period of time intervals, through cubic spline function, form the median-point-fit-curve with all the gained median points $m(t)$.
Step 8	Set $h(t) = x(t) - m(t)$.
Step 9	Repeat the above steps until $h(t)$ is an IMF, check in Table 1, and then set $c_i(t) = h(t)$.
Step 10	Compute the residue $r_i(t) = x(t) - c_i(t)$.
Step 11	Set $x(t) = r_i(t)$ and repeat the above steps to extract the next IMF until $r_i(t)$ is monotonic or constant.

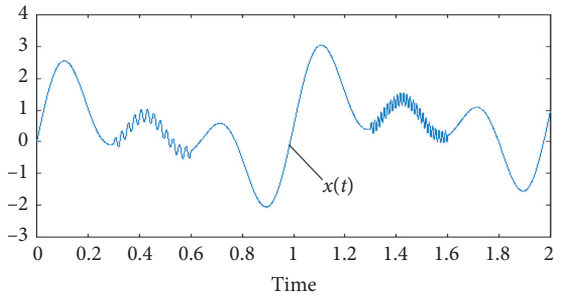

Figure 1: Synthetic signal waveform $x(t)$.

Despite the previous example [1] showing the EMD's accurate decomposition of a synthetic signal, the result above indicates that the mixed modes problem containing mixed components of the input signal cannot be decomposed successfully. Therefore, the same original signal $x(t)$ is taken as the input signal for the EEMD method for better comparison, shown as follows.

In Figure 3, it can be observed that when mixed modes occur, the signal components of different scales coexist in the same order of IMF. In other words, signal components with different frequencies coexist in the same order of IMF. From top to the bottom of Figure 3, each subfigure represents IMFs with ascending order produced by the EEMD method. As EEMD performing the signal $x(t)$, mixed modes can be reduced to a certain extent, but it cannot be eliminated fundamentally, and the decomposition result cannot reveal the signal characteristics and provide accurate information.

Note that MMD has multiresolution analysis and the advantages of signal analysis such as local adaptability, shown in Figure 4, where IMF1 is decomposed without the influence of mixed mode problem.

The process of the method for decomposing signals into each IMF is shown in Figure 4, demonstrating the advantage of self-adaptiveness and high efficiency in MMD.

The red curve in Figure 4 is the median-point-fit-curve $m(t)$, and the blue curve is the original signal $x(t)$; the difference between $x(t)$ and $m(t)$ can be obtained as an IMF if conditions meet equally (Table 1), denoted as $h(t)$. Even with a complex original signal in Figure 1, it can be noticed that imf1 $h(t) = x(t) - m(t)$ without obvious mixed mode.

Hence, the IMFs $h(t)$ equals the difference between the original signal $x(t)$ and the median-point-fit-curve $m(t)$. The MMD algorithm is operated in all five different composition processes in five different time intervals sorted by the

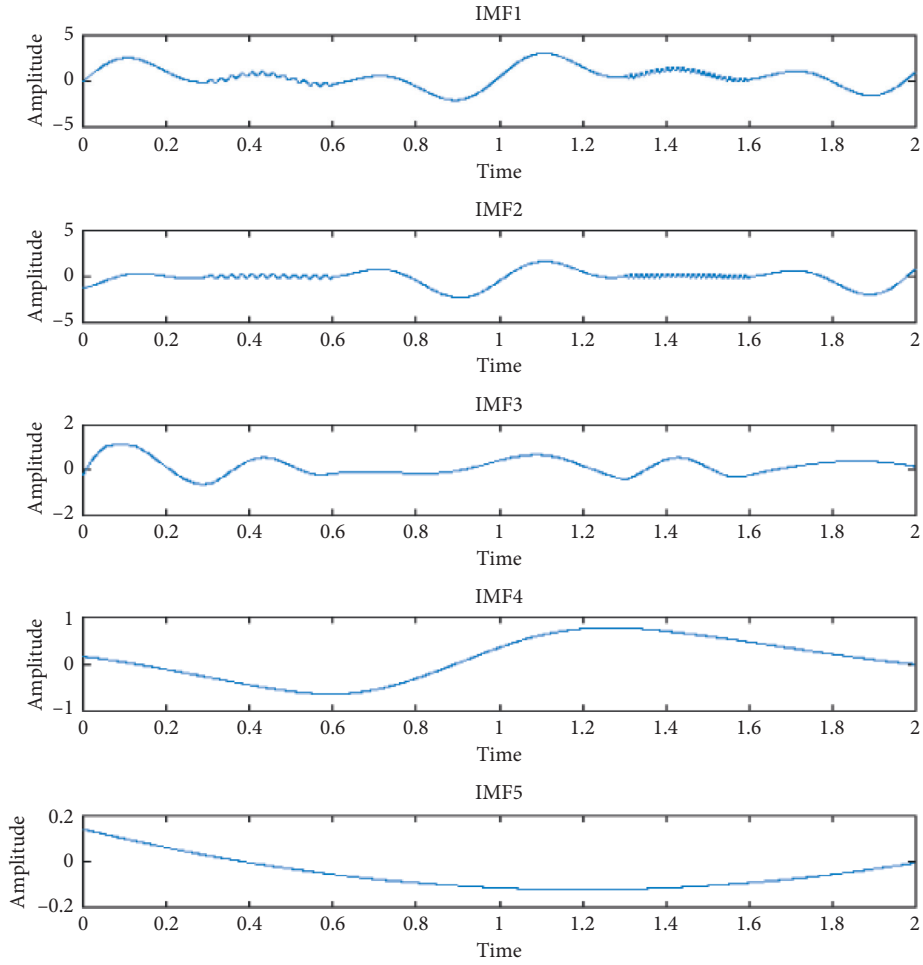

Figure 2: EMD result of signal $x(t)$.

ranking algorithm, in order to obtain IMF1-5, shown in Figure 5.

The result in Figure 5 demonstrates that the MMD method can effectively decompose the added interferences and normal signal into the correct constituent signals in various cases, alleviating mixed modes problem and being self-adaptive at the same time.

It can be seen from the results of IMFs in Figure 5 that MMD algorithm can decompose a series of IMFs from high to low frequencies, without the influence of mixed mode problem.

As the problem of mixed mode occurs, an IMF can cease to have physical meaning by itself, suggesting falsely that there may be different physical processes represented in a mode. In MMD, when acquiring IMF components, because too many iterations would damage the integrity of the signal and its physical meaning, the number of iterations needs to be limited. Therefore, the criterion to end iterations used in this method is already written in Tables 1 and 2 and Step 11 of Table 3.

Additionally, observing the differences of EMD and EEMD shown in Figures 2 and 3, the decomposition result of the EEMD method is better than that of the EMD method. However, EEMD takes three more steps to iterate out the final IMF component. Thus, the result of MMD using the same original signal $x(t)$ given in Figure 5 represents better mode decomposition.

Applying MMD to decompose $x(t)$ resulted in a series of IMFs, where the *imf*1-5 denote all the IMFs, showing a successful decomposition of four smoothly sinusoidal signals and single residual, accordingly. As can be seen, MMD can solve the problem of mixed modes well with the mode component very similar to the original signal. Comparing Figures 3–5, the IMFs decomposed by MMD is obviously more accurate than the decomposition results of EMD and EEMD. The frequency of each IMF is sequentially reduced, and the waveform transformation is more regular. It shows that MMD can avoid mixed mode because it could separate high-frequency and low-frequency components clearly and obtain the meaningful signal sufficiently. It can also prove that MMD maintains the adaptability in signal decomposition.

In the interim, the implementation flowchart of this proposed MMD method is shown in Figure 6. The $x(t)$ represents original signal in Figure 1. $c(t)$ stands for each of IMFs $h(t)$, and $r(t)$ denotes residue, which equals to $x(t) - c(t)$. The median-point-fit-curve m(t) is formed by cubic spline function. At first, identify all the local extrema of original signal $x(t)$ to obtain the local maxima and minima of

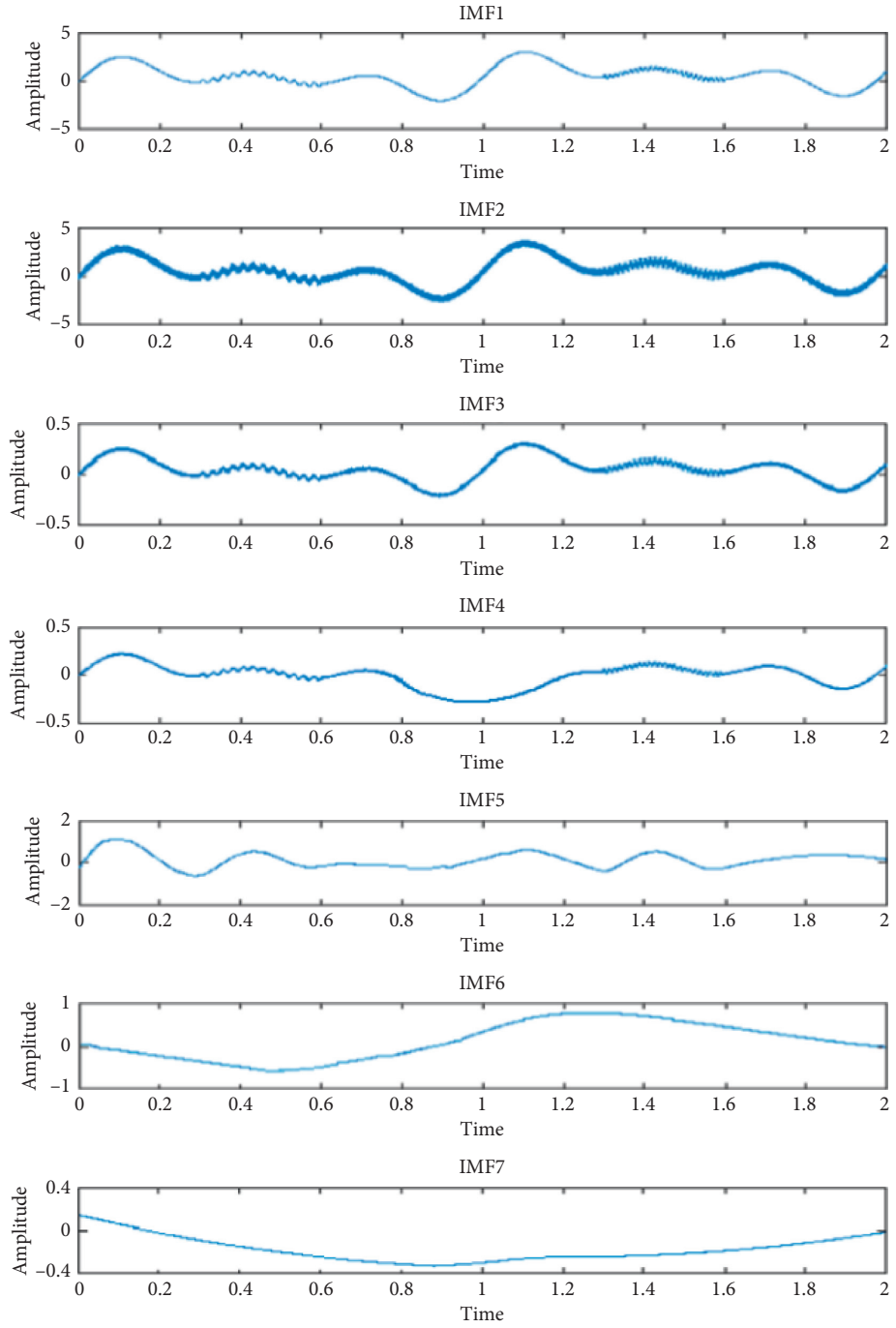

Figure 3: EEMD result of signal $x(t)$.

$x(t)$. Then, the time interval in all the adjacent extreme points is arranged in ascending order with sort-based inversion, selecting out the different frequency periods for MMD to operate, respectively. Check two conditions about the pre-set maximum of time interval Tmax of Table 2, then the cubic spline function is used to form the median-point-fit curve in each sorted time interval, and the median-point-fit curve obtained is processed in the next step according to the EEMD and EMD methods. Finally, the MMD algorithm achieves self-adaptive mode decomposition with the alleviation in mixed modes.

4. Motor Fault Recognition Experiments

The characteristic complexity in motor fault signal makes it hard to be detected. Generally, engineers and researchers adopt different diagnostic methods for different bearing faults of motors, but each one needs the separation from the decomposition and extraction of modes.

When a bearing fault occurs in an asynchronous motor, its vibration frequency will change significantly, and for different types of bearing faults, the characteristic frequency of the fault produced is also different.

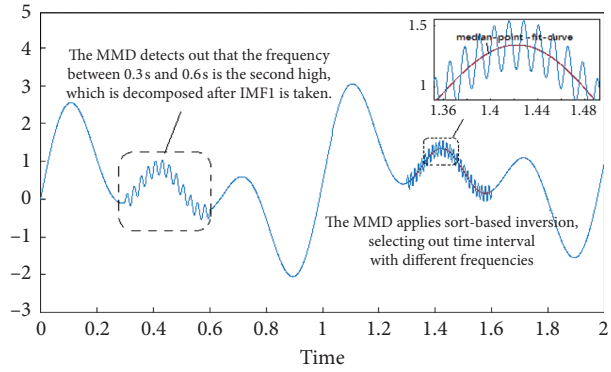

Figure 4: Synthetic signal waveform $x(t)$ for obtaining IMF1.

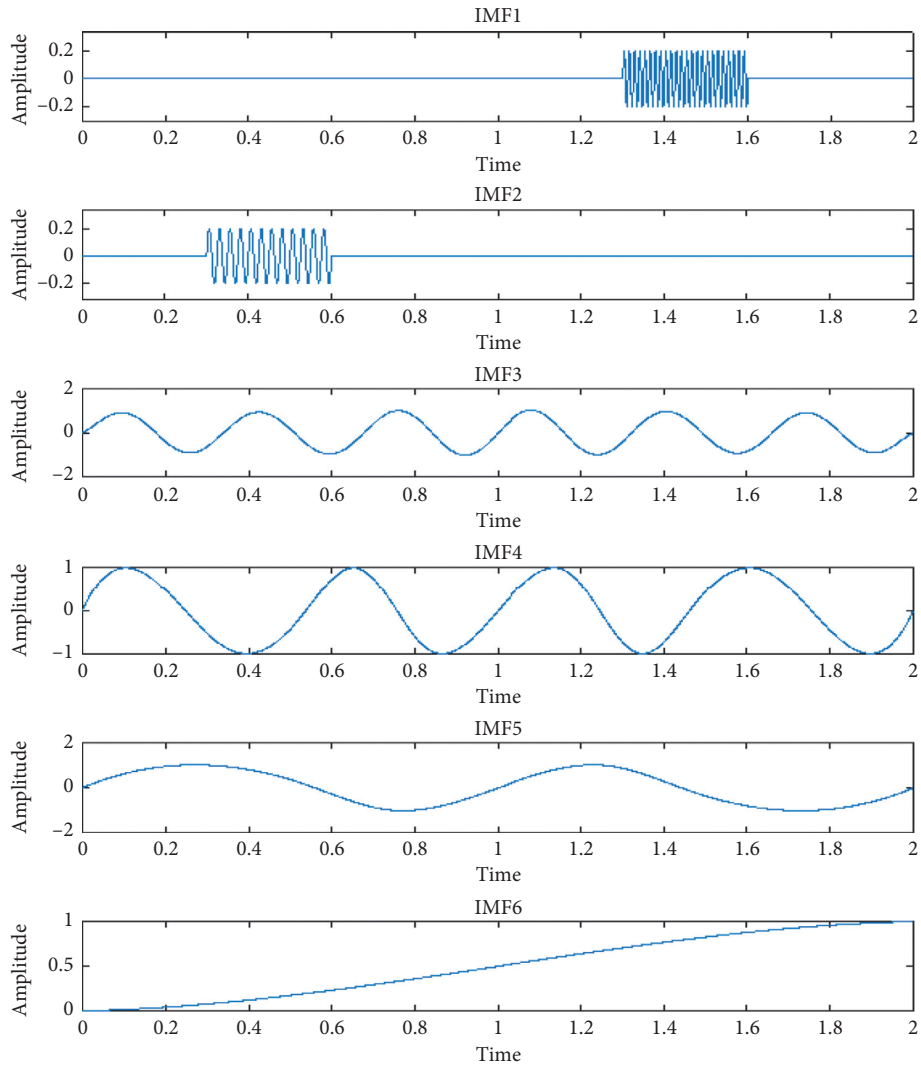

Figure 5: MMD result of signal $x(t)$.

Therefore, the type of bearing failure can be identified by the vibration characteristic frequency. The following is the vibration characteristic frequency formula of various bearing faults. The expression of outer ring fault fOD, inner ring fault fID, rolling element fault fBD, and cage fault fCD, are shown as follows [12]:

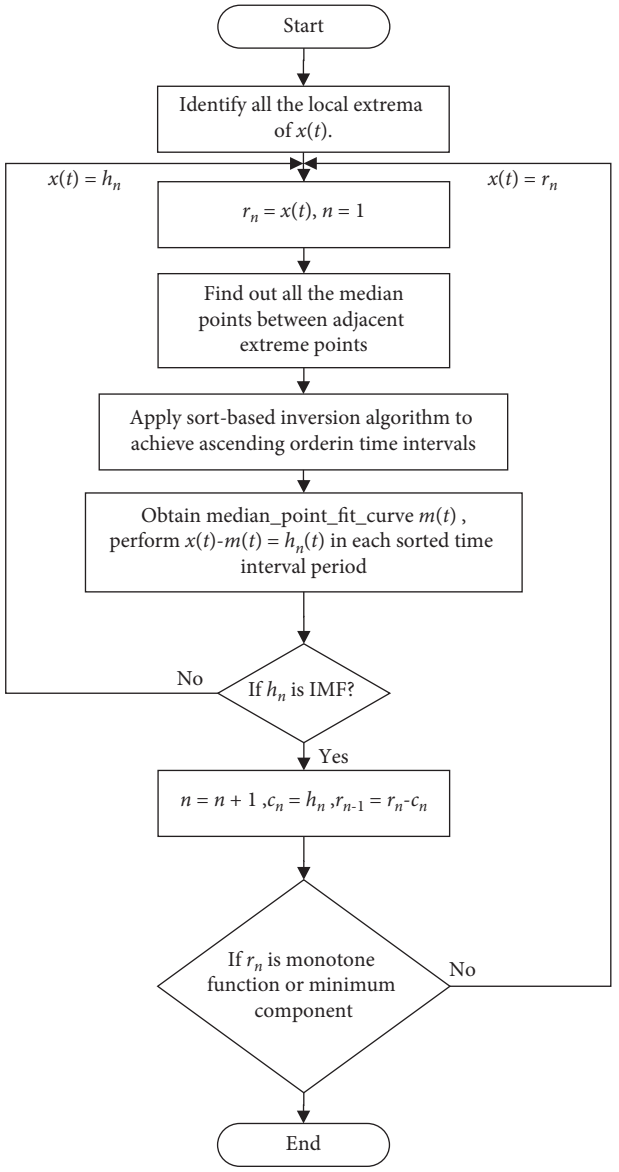

Figure 6: Implementation flowchart of MMD.

$$f_{\mathrm{OD}} = \frac{n}{2} f_{rm}\left(1 - \frac{d_b}{d_p}\cos\Phi\right), \tag{8}$$

$$f_{\mathrm{ID}} = \frac{n}{2} f_{rm}\left(1 + \frac{d_b}{d_p}\cos\Phi\right), \tag{9}$$

$$f_{\mathrm{BD}} = \frac{d_p}{2d_b} f_{rm}\left[1 - \left(\frac{d_b}{d_p}\cos\Phi\right)^2\right], \tag{10}$$

$$f_{\mathrm{CD}} = \frac{1}{2} f_{rm}\left(1 - \frac{d_b}{d_p}\cos\Phi\right), \tag{11}$$

where f_{rm} is the rotation frequency of motor, d_b and d_p are the diameter of the bearing rolling elements and the diameter of the bearing cage, respectively, n is the number of the bearing rolling elements, and Φ is the contact angle of rolling element.

As we can see above, the rolling element of motor rolling bearing fault is simulated and the time-domain waveform of the fault vibration signal is shown in Figure 7, where the vertical axis represents the vibration signal of the motor. For better observation, an enlarged view of Figure 7 during the time of zero to two seconds is presented in Figure 8. At the same time, the four IMF components (IMF1~IMF4) and one residual term (Res) obtained by adaptive MMD decomposition of the fault vibration signal are shown in Figure 9. Note that from the corresponding kurtosis value of each IMF component, we can conclude that since the kurtosis value of the IMF component of the 4th layer is the largest, the IMF4 component contains a lot of obvious fault characteristic information.

Therefore, the characteristics of the vibration signal as the rolling bearing outer ring in motor fault are verified, which demonstrates the effectiveness of the MMD method for the fault recognition.

Note that the MMD algorithm is able to alleviate the mixed modes problem in fault signal, where each IMF shows a certain periodicity. In this proposed method, the algorithm based on MMD and sort-based inversion is used to separate and alleviate the mixed modes. MMD decomposition of each quasi-margin term is re-decomposed to realize the self-adaptive function, making sure every IMF meets the conditions in Table 1. The result of EMD and MM obtained are both shown in Figure 9, illustrating through comparison with the conventional method that the algorithm successfully separated mixed modes problems in motor fault.

In Figure 9, the signal of IMF1 is completely extracted in the MMD method, while the EMD method still has mixed mode problem. Note that the resonance occurs with specific resonance frequency, and we manage to analyze with Hilbert–Huang spectrum for further needs of fault recognition.

In order to respond to the relationship between time-frequency-amplitude more intuitively, the three-dimensional Hilbert spectrum based on the information from the above IMFs is drawn in Figure 10. In Figure 10, there are fluctuations in the low-frequency part, but basically no energy distribution on the high-frequency part, which can be seen as linearly distributed and stable.

For better observation in the low-frequency part, comparative IMFs marginal spectrums of EMD and MMD in motor rolling bearing fault are given in Figure 11. The decomposition result of MMD has 5 IMFs. The IMFs contain enough physical meaning which are called effective intrinsic functions (EIMF). False intrinsic mode function (FIMF) components denote no physical meaning in IMFS. As can be seen in Figure 11, the result from EMD of Figure 11(a) conducts more numbers of FIMFs than MMD, which means the MMD method has better performance, particularly in fault recognition of rolling element bearings.

It can be seen from Figure 11(b) that the largest amplitude is around 0.35 with the frequency of near 38 Hz. According to theoretical calculation in equation (9), the inner ring is faulty with the calculated frequency of 37.6 Hz. Thus, the frequency near 38 Hz occupies the main

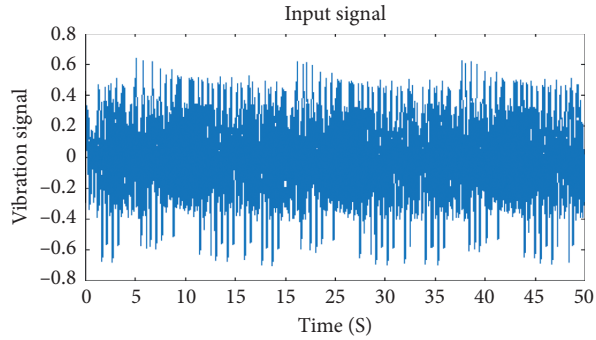

Figure 7: Synthetic signal waveform of motor rolling bearing simulated fault.

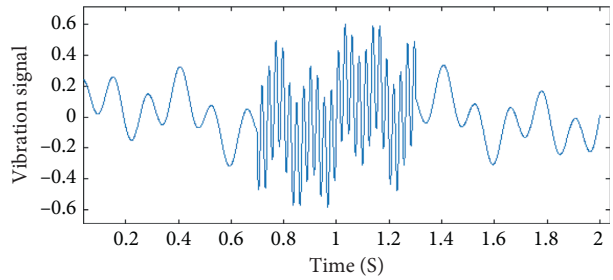

Figure 8: Synthetic signal waveform of motor rolling bearing simulated fault from the time of 0 s to 2 s.

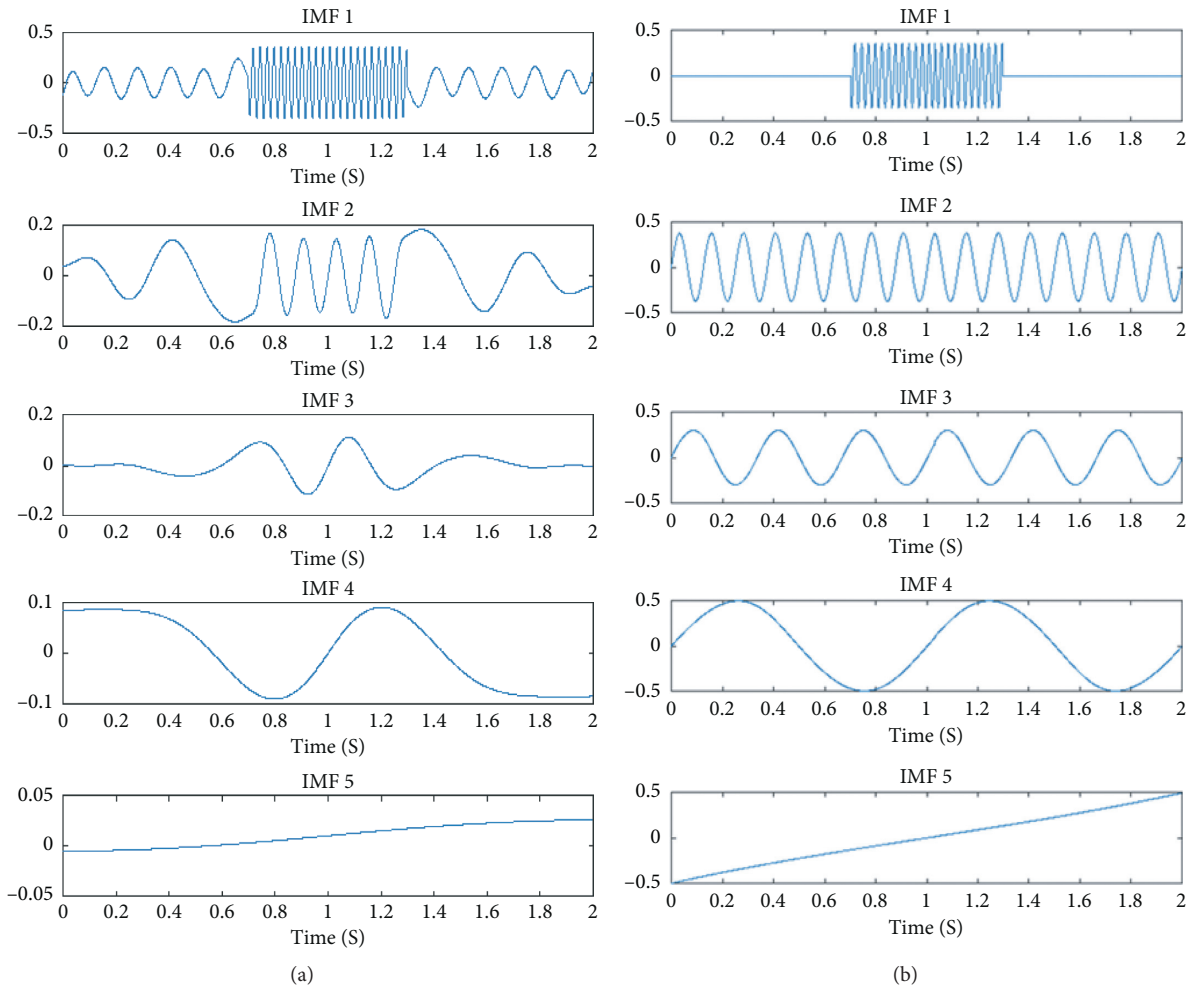

Figure 9: Result of signal of motor rolling bearing simulated fault. (a) EMD method; (b) MMD method.

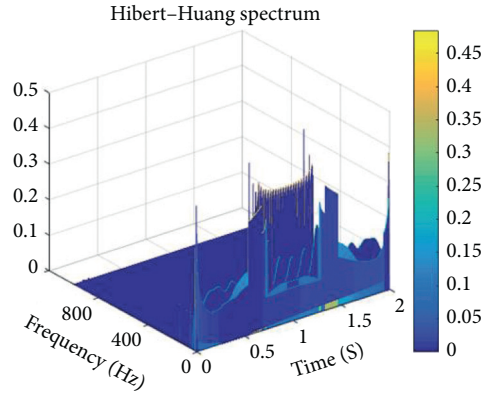

Figure 10: Hilbert–Huang spectrum waveform of motor rolling bearing simulated fault.

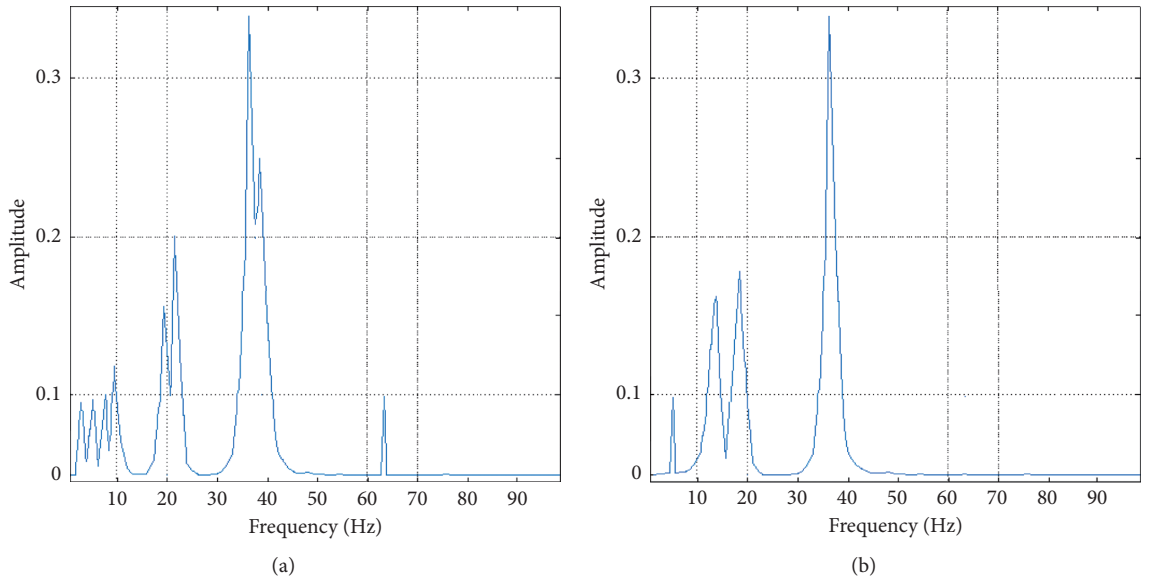

Figure 11: Each IMF marginal spectrum of MMD in motor rolling bearing simulated fault. (a) EMD method; (b) MMD method.

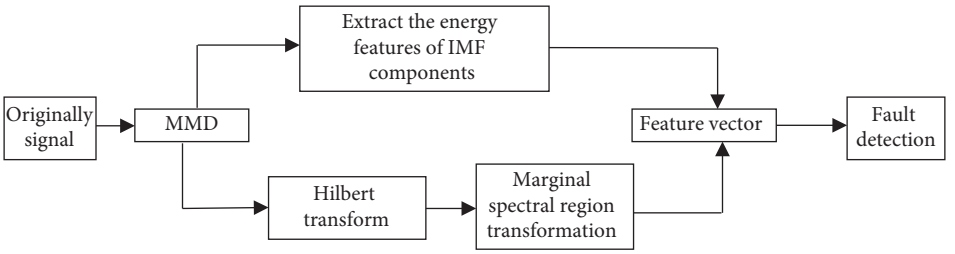

Figure 12: Process of MM when applied to fault recognition.

components, representing ability gathering, which proves obvious fault information and can be treated as a motor rolling bearing fault. That is, the MMD method can effectively extract the signal feature effectively and avoid the mixed modes problem.

Figure 12 shows the whole process of MMD applied in practice for extracting the motor fault; thus, the detected feature vector verifies the effectiveness of the proposed algorithm.

5. Conclusions

A fault recognition method for motor rolling bearing fault is put forward in this paper, which is based on a novel median-

point mode decomposition (MMD) with sort-based inversion algorithm. The MMD method is not only suitable for analyzing complex multicomponent signals but also chosen to precondition the vibration signal of the roller bearing to produce a set of IMF components. For the fact that the vibration signal is nonlinear and unstable, the MMD method keeps the algorithm self-adaptive for sorting out each variation of the extreme points interval with better and specific mode decomposition. Comparison simulations and experiments are operated to highlight the advantages of MMD in dealing with mixed mode problem in nonlinear signals.

In summary, MMD is a better choice when the signal needs time-frequency analysis, especially when the signal is nonlinear and nonstationary. The proposed method MMD keeps the advantages of EMD and EEMD and avoid mixed mode, which makes it capable of capturing the features of the signal in motor rolling bearing fault accurately. [13–18]

Data Availability

The data used to support the findings of this study are available from the corresponding author upon request.

Conflicts of Interest

The authors declare that they have no conflicts of interest.

Authors' Contributions

Ganzhou Yao and Bishuang Fan contributed equally to this work.

Acknowledgments

This work was supported by the National Science and Technology project called "Research on Coordinated Control methods of Single-Phase-to-Ground Fault Flexible Arc Suppression and Protection for Distribution Networks" (No. 51877011).

References

[1] N. E. Huang, Z. Shen, S. R. Long et al., "The empirical mode decomposition and the Hilbert spectrum for nonlinear and non-stationary time series analysis," *Proceedings of the Royal Society of London. Series A: Mathematical, Physical and Engineering Sciences*, vol. 454, no. 1971, pp. 903–995, 1998.

[2] R. Gabriel and P. Flandrin, "One or two frequencies? The empirical mode decomposition answers," *IEEE Transactions on Signal Processing*, vol. 56, no. 1, pp. 85–95, 2008.

[3] K. D. Seger, M. H. Al-Badrawi, J. L. Miksis-Olds, N. J. Kirsch, and A. P. Lyons, "An empirical mode decomposition-based recognition and classification approach for marine mammal vocal signals," *The Journal of the Acoustical Society of America*, vol. 144, no. 6, pp. 3181–3190, 2018.

[4] C. Amo, L. de Santiago, R. Barea, A. LópezDorado, and L. Boquete, "Analysis of gamma-band activity from human EEG using empirical mode decomposition," *Sensors*, vol. 17, no. 5, p. 989, 2017.

[5] Y. Li, J. Liu, and Y. Wang, "Railway wheel flat recognition based on improved empirical mode decomposition," *Shock and Vibration*, vol. 2016, Article ID 4879283, 14 pages, 2016.

[6] J. Zheng, J. Cheng, and Y Yang, "Partly ensemble empirical mode decomposition: An improved noise-assisted method for eliminating mode mixing," *Signal Processing*, vol. 96, pp. 362–374, 2014.

[7] G. Li, Z. Yang, and H. Yang, "Noise reduction method of underwater acoustic signals based on uniform phase empirical mode decomposition, amplitude-aware permutation entropy, and pearson correlation coefficient," *Entropy*, vol. 20, no. 12, p. 918, 2018.

[8] J.-C. Nunes and E. Delechelle, "Empirical mode decomposition: Applications on signal and image processing," *Advances in Adaptive Data Analysis*, vol. 1, no. No. 1, pp. 125–175, 2009.

[9] C. Wang, H. Li, and D. Zhao, "A preconditioning framework for the empirical mode decomposition method," *Circuits System Signal Process*, vol. 37, no. 12, pp. 5417–5440, 2018.

[10] R. T. Rato, M. D. Ortigueira, and A. G. Batista, "On the HHT, its problems, and some solutions," *Mechanical Systems and Signal Processing*, vol. 22, no. 6, 2008.

[11] R. Ho and K. Hung, "A comparative investigation of mode mixing in EEG decomposition using EMD, EEMD and M-EMD," in *IEEE 10th Symposium on Computer Applications & Industrial Electronics (ISCAIE)*, pp. 203–210, Penang, Malaysia, April 2020.

[12] X. Hu, S. Peng, and W.-L. Hwang, "EMD revisited: A new understanding of the envelope and resolving the mode-mixing problem in AM-FM signals," *IEEE Transactions on Signal Processing*, vol. 60, no. 3, pp. 1075–1086, 2012.

[13] T.-L. Kung and C.-N. Hung, "Estimating the subsystem reliability of bubblesort networks," *Theoretical Computer Science*, vol. 670, pp. 45–55, 2017.

[14] G. Xua, Z. Yangb, and S. Wang, "Study on mode mixing problem of EMD," in *Proceedings of the Joint International Information Technology, Mechanical and Electronic Engineering Conference*, Chongqing China, May 2016.

[15] Y. R. Du, L. H. Chen, and H. Jin, "A new view of mode mixing phenomenon," *Applied Mechanics and Materials*, vol. 532, pp. 134–137, 2014.

[16] Y. Kopsinis and S. McLaughlin, "Investigation and performance enhancement of the empirical mode decomposition method based on a heuristic search optimization approach," *IEEE Transactions on Signal Processing*, vol. 56, no. 1, 2008.

[17] Y. O. Adu-Gyamfi, N. O. Attoh-Okine, and A. Y. Ayenu-Prah, "Critical Analysis of different hilbert-huang algorithms for pavement profile evaluation," *Journal of Computing in Civil Engineering*, vol. 24, no. 6, 2010.

[18] B. Xu, Y. Sheng, P. Li, Q. Cheng, and J. Wu, "Causes and classification of EMD mode mixing," *Vibroengineering Procedia*, vol. 22, pp. 158–164, 2019.